Volvox Inversion Mechanics
Research Report
Solid Mechanics
ES240

Ben M. Jordan

December 17, 2008

Abstract

The genus Volvox is comprised of several species of communal multi-cellular chlorophytes which exhibit a series of interesting morphogenetic events during their developmental cycle. In *Volvox carteri*, the inversion event is interesting in that after several rounds of cell division from a single cell, the glycoprotein filled, spheroidal plakea completely inverts itself thorough of series of highly coordinated genetic, kinetic and mechanical interactions[4, 3, 7, 5]. This dramatic coming of age of the adult colony is beginning to be understood from a developmental viewpoint, with descriptive data on the phenomena for both wild-type and mutants, as well as the distribution of relevant gene products now available. Herein, I examine the experimental data, and propose a mathematical model to describe this process, taking into consideration both the chemical kinetics and the tissue mechanics of the colony. The resulting system of coupled equations is solved in an approximated geometry of the mature gonidia, using the finite element method (FEM). Results are compared with the observed data, as well as exact solutions for idealized parametrization.

Background

The life cycle of *Volvox carteri* begins as single celled gonidia; a reproductive cell that develops into a fully grown adult. These gonidia are the reproductive cells produced and fostered to maturity by the adult. Even before being birthed from the parent, the cell undergoes regular, but asymmetric divisions, resulting in a 64-celled spheroidal mature gonidia, comprised of somatic, and its own gonidial precursor cells (See Figure 1). In total, each individual goes through 11-12 rounds of volume increase and division during its lifetime. To further convolute the line between individuality and community, an anterior/posterior axis is formed by concentration gradients during development.
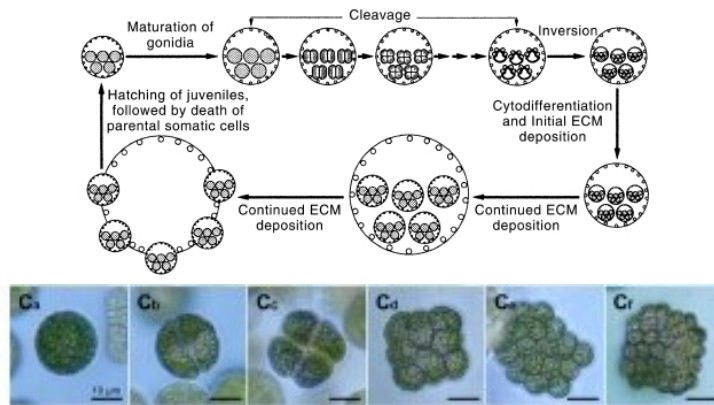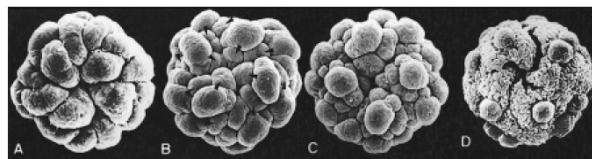
Figure 1: Life cycle and 5 cleavage cycles

After 5th cleavage cycle, the individual has 32 cells. At this point, half of the anterior 16 cells differentiate into gonidia precursors. The gonidia precursors undergo 3 more rounds of division, resulting in 64 gonidia before the inversion event occurs. The somatic cells divide 6-7 more times, depending on environmental conditions, resulting in 3072 maximum cells pre-inversion. Somatic cells are $\frac{1}{10}th$ of the volume of the gonidia, and are connected via 25,000 cytoplasmic bridges, forming a continuous epithelial sheet. The only unconnected region of this network of cells is at the anterior end, where the phialopore forms. This the swastika-shaped opening forms between the 3rd and 4th round of cleavage. At this point, multiple contraction waves pass through the cell colony, from the anterior to posterior ends, after which the phialopore (located at the anterior end as well) breaks apart at four lips, and begins to curl outward. The generation of this negative curvature is caused by the change in form of the cells near the philopore, as they change from spindle-shaped to flask-shaped and back to spindle-shaped. (See Figure 2).

As the wave change reaches the posterior half of the colony, the posterior end snaps through the opening created, and the lips meet each other at what is now the new posterior half and rejoin. During this process, the pre-gonidial cells, which were once on the outside of the colony in the anterior half, are transported to the posterior inside of the new adult spheroid. The flagellar extensions from the somatic cells, which were pointed inward in the immature gonidia, are now on the outside, allowing for locomotion of the adult spheroid. The entire process takes approximately 45 minutes.
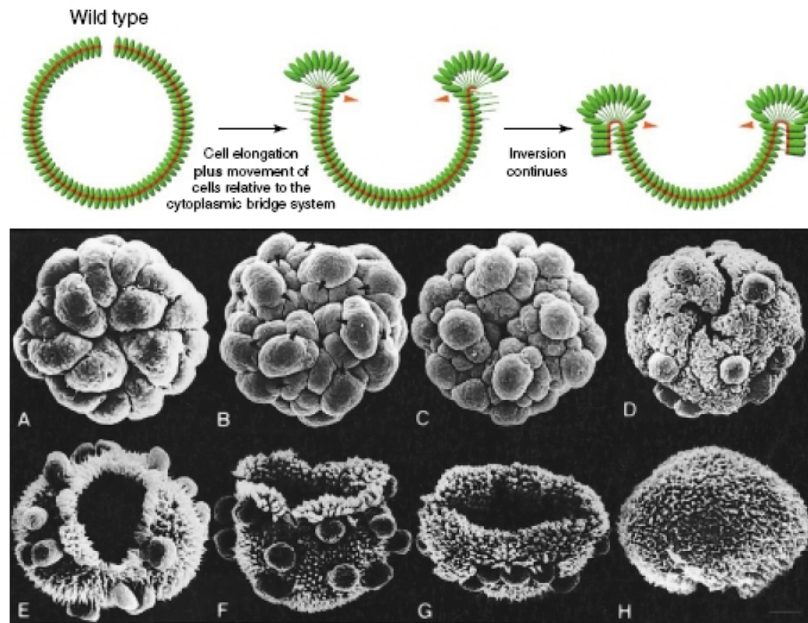
Figure 2: Inversion, pictorial and actual (SEM)[8]

Several mutants, induced by genetic modification, and/or chemical/mechanical stimulation of the developing organism exist. One mutant form, induced by application of cytochalasin, halts or terminates the inversion process, depending on when the application is made during the process. This has been shown to be due to the ability of cytochalasin to inhibit the movement of cytosolic bridges between cells; a process crucial for the transition from spindle- to flask-shaped[8, 7] described above. Another mutant caused by the creation of a second philopore slit at the posterior half causes the inversion to begin from both ends, resulting in a toroidal adult. These phenomena represent manipulation of the mechanical and chemical interactions that are coordinated to complete inversion, and are thus predictable by a model that correctly describes the wild-type inversion process.

Volvox is useful as a model system for studying multicellular tissues and epithelial sheet movements, which occur in processes such as gastrulation and notochord formation in vertebrates, such as humans. There is rich quantitative literature with genetic, developmental, and evolutionary data readily available, and a small, but vibrant research community interested in it. As discussed above, there are several developmental mutants and techniques are available for experiment, and for hypothesis testing. Using this system, I can begin to answer questions about the inversion process. Does the geometry change of the anterior somatic cells account for the entire inversion? Does the posterior actomyosin contraction account for the inversion? What role does geometry play in this

process? What role do protein kinetics play in this process?

Mathematical Model

I begin by considering a single cell as it undergoes the contraction and elongation process into a flask-shaped cell. As these cells contract on one end, and expand on the other, they apply force to each other where they meet, causing the outward curling near the phialopore that is observed in figure 2. Since we know the exact sizes and deformations of these cells, this simulation helped me find a reasonable Young's modulus and Poisson ratio for the next steps. The geometry for this single ellipsoidal cell is shown in figure 4a, and the standard equations of solid mechanics, with a Hookean material model are used (figure 5). While the cell is actually a fluid filled, and matrix-rich, this is a reasonable first approximation for understanding the beginning of the inversion process.

Next, I examine how a line and an arc of these cells undergoing a contractile wave deforms. By treating the line/arc as a continuous piece of material, and using the plane strain approximation, we can observe what a number of the cells from the first part contracting as a wave passes through them does. The geometry of this line and arc is seen in figure 4b and 4c.

Now, I examine the three-dimensional geometry. Since it has been shown that one can remove the entire anterior half and the posterior half still inverts, I first consider the posterior half-sphere only. This is truly the novel part of the project, and was the most interesting part to describe. As before, we use the standard equations of solid mechanics, as shown in figure 4. In order to understand this aspect of the inversion process, I constructed rubber models of various geometries and materials of half-spheres, as shown in figure 3. While the scale of the inversion of *Volvox* itself is much smaller and the time scale much longer, I thought it crucial to correctly simulate an object I could repeatedly observe. For this reason, this project could have been retitled "Inversion of spherical membranes".

For the FEM model, I consider 3 different geometries that are exactly a half-sphere, a half-sphere which has been truncated from the mid line towards the apex by 0.005 m, and one that has been truncated by 0.025 m as shown in figure 4d, 4e, 4f.
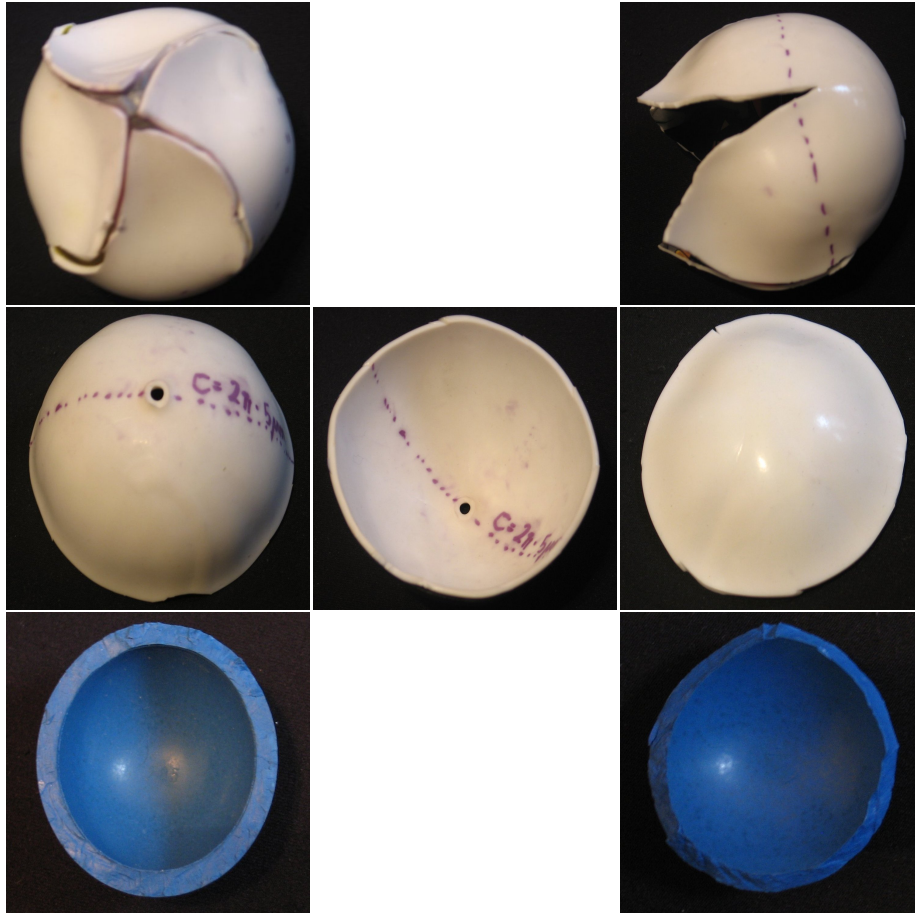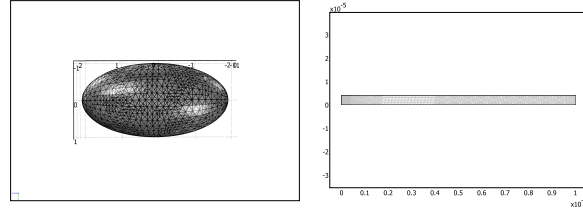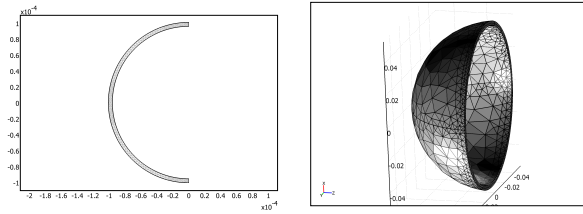
Figure 3: Rubber models: The full Volvox-like rubber model, the half-sphere, and the half-half-sphere.
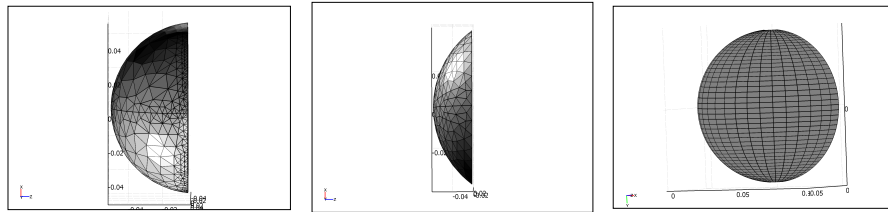
(a) Single cell

(b) Line of cells

(c) Arc of cells

(d) Posterior half

(e) Truncated posterior half   (f) Truncated posterior half   (g) Truncated posterior half

Figure 4: Geometry and meshing of simulated experiments.

Contraction Functions

The contraction, as well as the material properties of the wall are controlled by the concentration of various chemical factors within the organism[6, 5, 2, 1]. These range from simple ions, such as calcium, to large protein complexes, which both either diffuse or remain in a single cell. During the interim of this

Momentum balance:	$\frac{\partial \sigma_{ij}}{\partial x_j} + b_j = \rho \frac{\partial^2 u_i}{\partial t^2}$
Strain-displacement*:	$\varepsilon_{ij} = \frac{1}{2}\left(\frac{\partial u_i}{\partial x_j} + \frac{\partial u_j}{\partial x_i}\right)$
Hooke's law:	$\varepsilon_{ij} = \frac{1+\nu}{E}\sigma_{ij} - \frac{\nu}{E}\sigma_{kk}\delta_{ij} + \alpha_1 \Delta c_i$
Reaction-diffusion:	$\frac{\partial \mathbf{c}}{\partial t} = D\nabla^2 \mathbf{c} + f_R(c_i, \mathbf{x})$
Young's modulus (E):	$10^5 Pa$
Poisson ratio (ν):	0.49
Inner radius of spheroid (R):	$4.5 \cdot 10^{-6}$ m
Thickness of spheroidal shell (δ):	$0.5 \cdot 10^{-6}$ m
Contraction amplitude coefficient (α_1):	-1
Contraction duration coefficient (α_2):	200
Contraction length in Z coefficient (α_3):	0.125

*Large deformation was used in the final formulation.

Figure 5: Equations and parameters used

project, the details of the relevant kinetic components will be explored, likely resulting in several species which interact with each other. This system of reactions is modeled using Michaelis-Menten kinetics, and thus is represented by a reaction-diffusion-advection system, where $\mathbf{c}$ is the vector of the chemical species considered, D is the diffusion coefficient, and $f_R(c_i, \mathbf{x})$ is a per-species, location specific, nonlinear reaction function. As the final result of this reaction-diffusion system will be an exponential wave, I simply prescribe this wave function in some of the simulations, as noted. I hope to actually fully couple the two in a future work.

In order to model a wave of contraction, a component analogous to thermal expansion of the stress-strain relation was used. For the two-dimensional simulations above, in which cellular elongation played a role, and a sheet of cells curled, I used the following travelling modulated wave

$$\alpha_1 \cdot \sin\left(\alpha_2 \cdot X \cdot \pi\right) \cdot e^{-\alpha_2 \cdot Y} \cdot e^{-(t-1+\alpha_3 \cdot X)}$$

For the three dimensional half-sphere, I modeled a contraction of the material as a exponentially decaying wave as follows:

(a) $e^{-\alpha_3(x+R)}$ (b) $e^{-(-\pi+\alpha_2\pi t)^2}$ (c) $e^{-((R+\delta-r)/\delta)^2}$
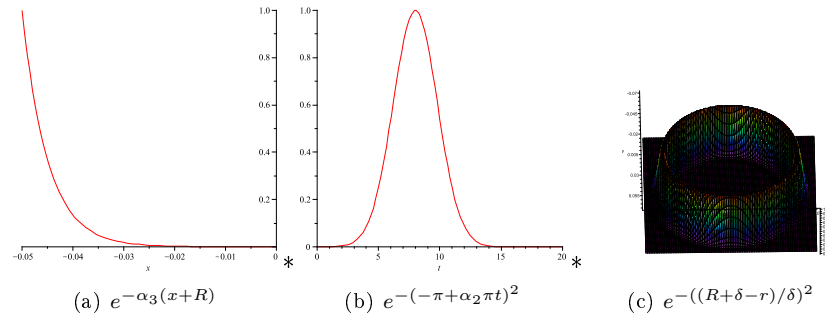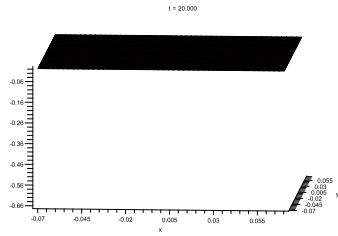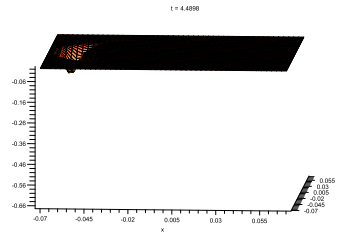
Figure 6: The construction of the contraction function: $c(x, y, z, t) = e^{-\alpha_3(x+R)} * e^{-(-\pi+\alpha_2\pi t)^2} * e^{-((R+\delta-r)/\delta)^2}$
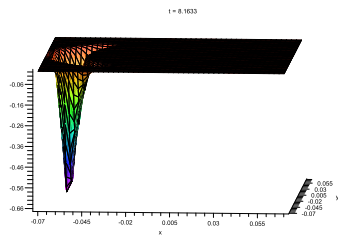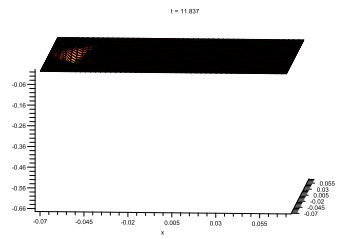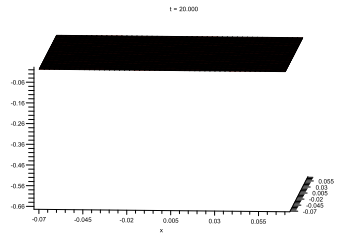
(a) t=0

(b) t=4

(c) t=8

(d) t=12

(e) t=20

Figure 7: The contraction function: a two-dimensional version of $c(x, y, z, t) = e^{-\alpha_3(x+R)} * e^{-(-\pi+\alpha_2\pi t)^2} * e^{-((R+\delta-r)/\delta)^2}$ at various times.
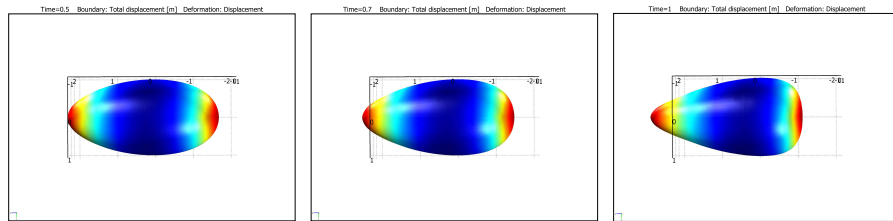
Results

Cell elongation via contraction

Figure 8: The contraction of a single cell on the left side caused a bulge on the right side. When a number of these cells are near each other, they exert forces on each other where the bulges meet.

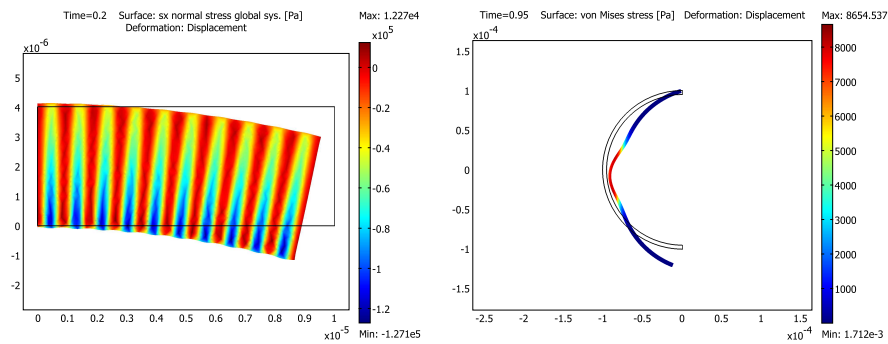## Contraction of anterior line/arc of cells

Figure 9: Putting a number of these elongating cells together in a line or an arc, and applying a contraction gives us a deformation above.

This test showed that the deformation could occur by this mechanism with the known material parameters. Using the plane strain approximation, a slice of a long arc of cells was subjected to a contraction function in 2D. The resulting deformation was useful in understanding the method for inversion, but the

true snap-through instability could only be realized in the three-dimensional geometry.

Inversion of a half sphere

As described above, the problem of the inverting Volvox was generalized to that of a inverting rubber half-sphere, in order to understand more about the deformation involved. Figure 10 shows the strains realized in all three directions during the maximum of the contraction function on the full half sphere. These values are within a valid range, and are as expected for this type of contraction. Figure 11 examines the stresses at the same time point in the simulation. Again these values are in a valid range, and they begin to tell us a bit about the nonlinear nature of stress in the deforming sphere. Figure 12 plots the deformation of the arc shown in red at the height of the contraction function. This curve is well known and is observed in processes that are opposite to contraction, such as outgrowth as well. Lastly, the deformation of several nodal points was plotted in Figure 13, and from this we can observe the expected curling of the membrane at the membrane as the contraction reaches its height at the apex.

Based on the initial experiments performed, especially what was learned from the plane strain approximation results in the line and arc of cells, the full 3D geometry was absolutely necessary to capture the effects of the geometry on the snap-through instability. Using a perfect half-sphere, I was unable to obtain a convergent solution due to a particularly stiff problem. After examining the stress, strain and displacements observed in these experiments, it was hypothesized that there is either a singularity reached at the apical node, or along the circumferential ring at the A/P mid-line. Several more experiments were done to test this theory, including the use of higher order elements and customized, high-resolution meshing in these regions.

As simulation progressed on the 3D geometry, I continually ran into convergence problems at the point at which the bi-stability arose. To see if there was error creeping into the solution due to low-order interpolation. Consequently, I used linear, quadratic, cubic, and even quartic elements and compared the results. While the difference between the curvature obtained between linear and quadratic elements was obvious, the difference between the solution using cubic and quartic elements was only slight, thus quadratic shape function were used in all results.

Regardless of the order of the shape functions used or the mesh type, the solution failed to converge due to the nonlinear solver. By examining the time-stepping algorithm in Comsol, I was able make the stepping more strict, in the sense that large jumps were not made between steps in the solution. This is important, due to the sensitive dynamic nature of the problem. Prior to making this modification to the solver algorithm, the solver may jump up to 10 time steps between linear system solution. basically, it was jumping over the bifurcation point.

After consulting the rubber models again, several more simulations were done using the most easily inverted geometry, the half-half-sphere. As shown in
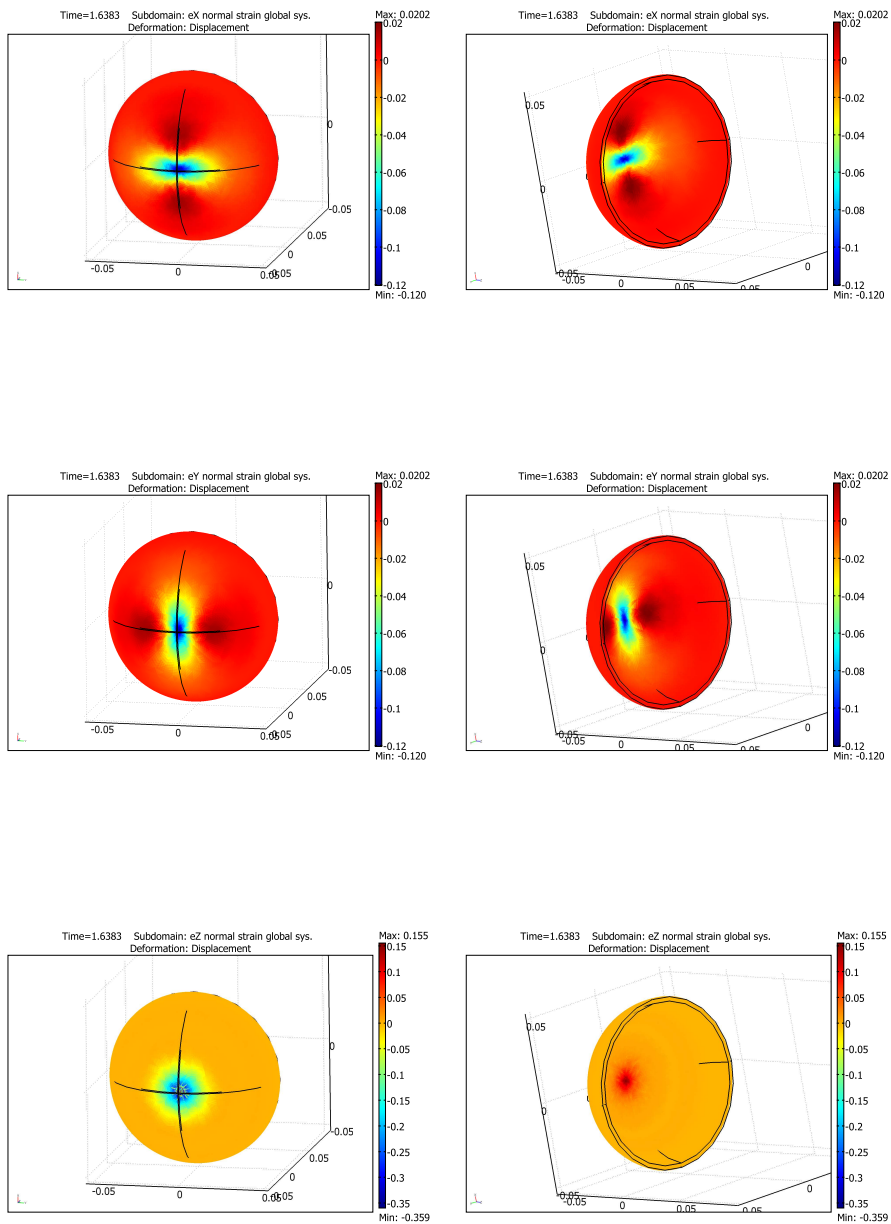
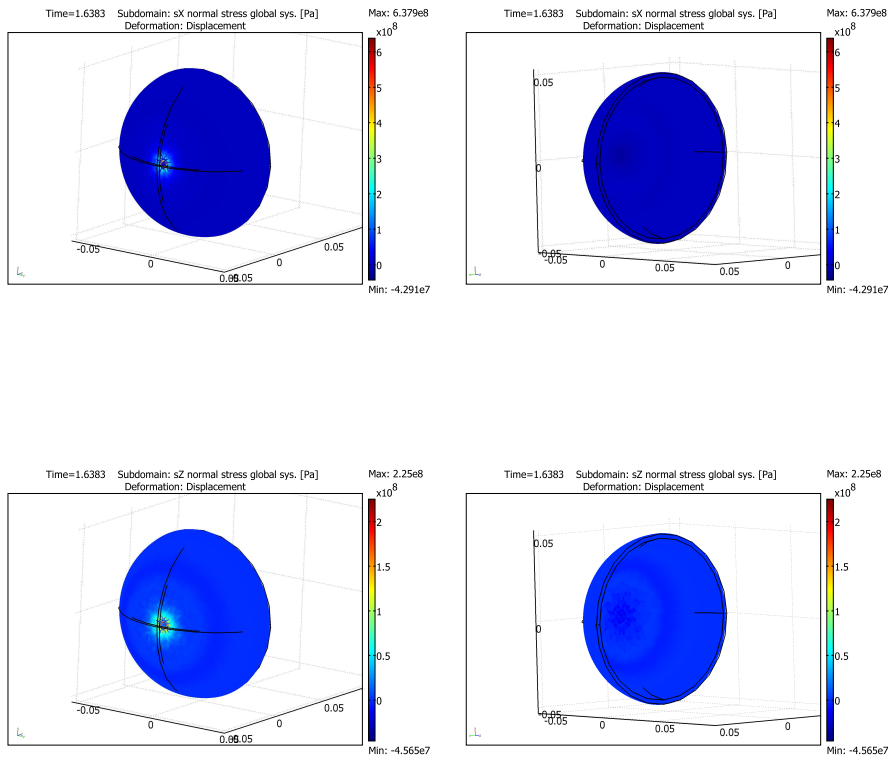Figure 10: Strains caused by the contraction function

Figure 11: Stresses caused by the contraction function. Stresses in X,Y are exactly the same, and thus only X is shown.
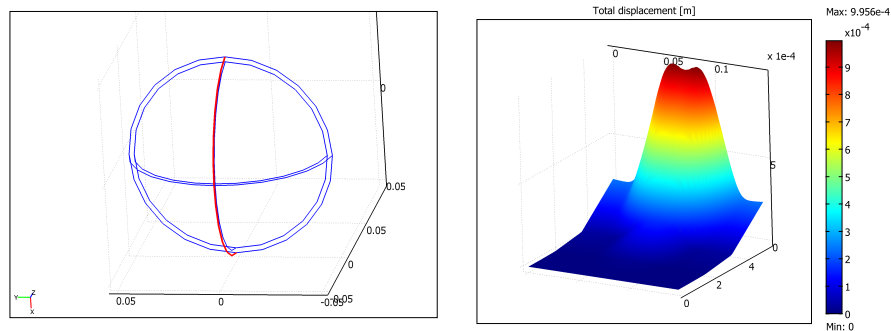
Figure 12: Displacement along the arc length of the hemisphere (red) plotted over time

figure 14, by (i) slowing the contraction function down to occur over a longer period, (ii) forcing the time-step to be small, and (iii) using a geometry that does not create a bifurcation point, I was able to arrive at an inverting membrane.

Figure 15 details the apical and circumferential nodal displacements, and we can see nicely see the point at which inversion occurs (just after t=6.3).

Future Work

There is much work left to be done here. In the rubber half-sphere alone, a complete variation of parameters study could be done which could help to elucidate the relationship between the thickness of the membrane, the amount of the sphere that is included in the inversion, and the material properties. During this process, a comparison of stress, strain, and pressure results must be made to see if they are of the right magnitude.

From here, we must return to the reality of the *Volvox*. To begin with, the mode of contraction and elongation of the cells must be better understood. It is quite likely that the method of contraction that we observe in the posterior end is the same as that in the interior end, but without the phialopore. Secondly, since the material is not rubber, and is a interconnected cell network which share cytoplasm, as well as extracellular matrix, the Hookean solid material model may not be appropriate. A viscoelastic model may be more appropriate, or a fluid-filled Hookean membrane. Additionally, as the scale of the rubber models is much different, we must consider that the snap-through instability observed in the rubber ball models may not be the mechanism that pops the rear through on the real organism. While it is likely similar, we need to take into account the change in scale, and consider how this effects the role of inertia
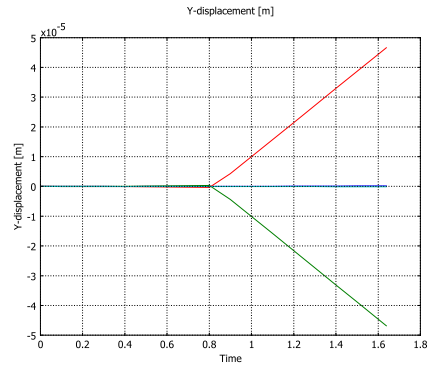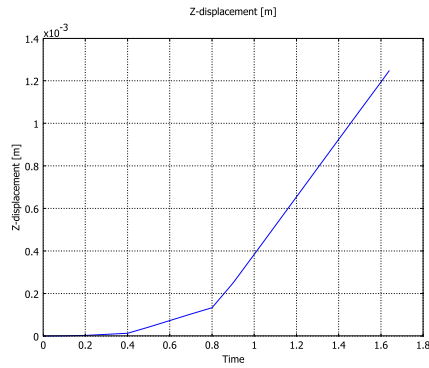
14
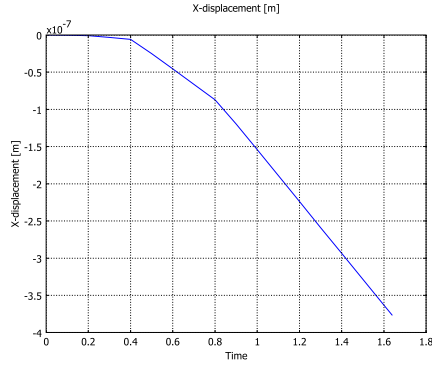
(a) X displacement at apex
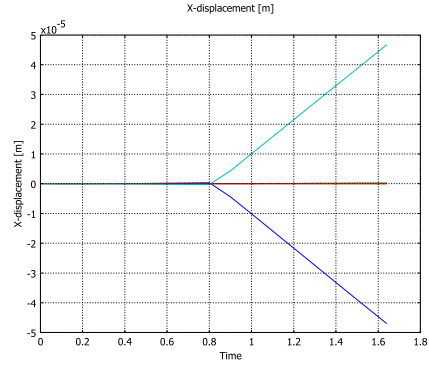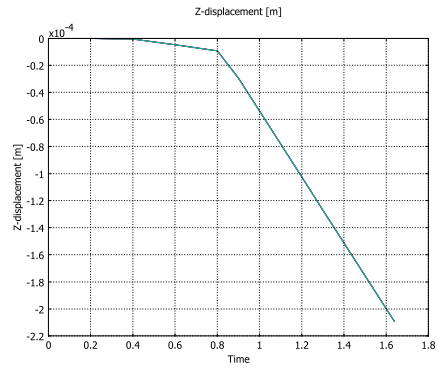
(b) X displacement at midline
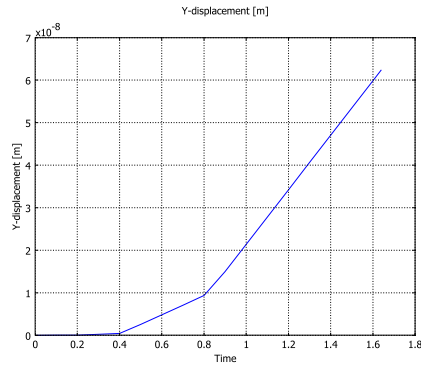
(c) Y displacement at apex

(d) Y displacement at midline

(e) Z displacement at apex

(f) Z displacement at midline

Figure 13: (1-3) Displacements at apical node {a,c,e}=(0, 0, −0.05) and circumferential nodes {b,d,g}= (0.05, 0, 0), (0, 0.05, 0), (−0.05, 0, 0), (0, −0.05, 0)
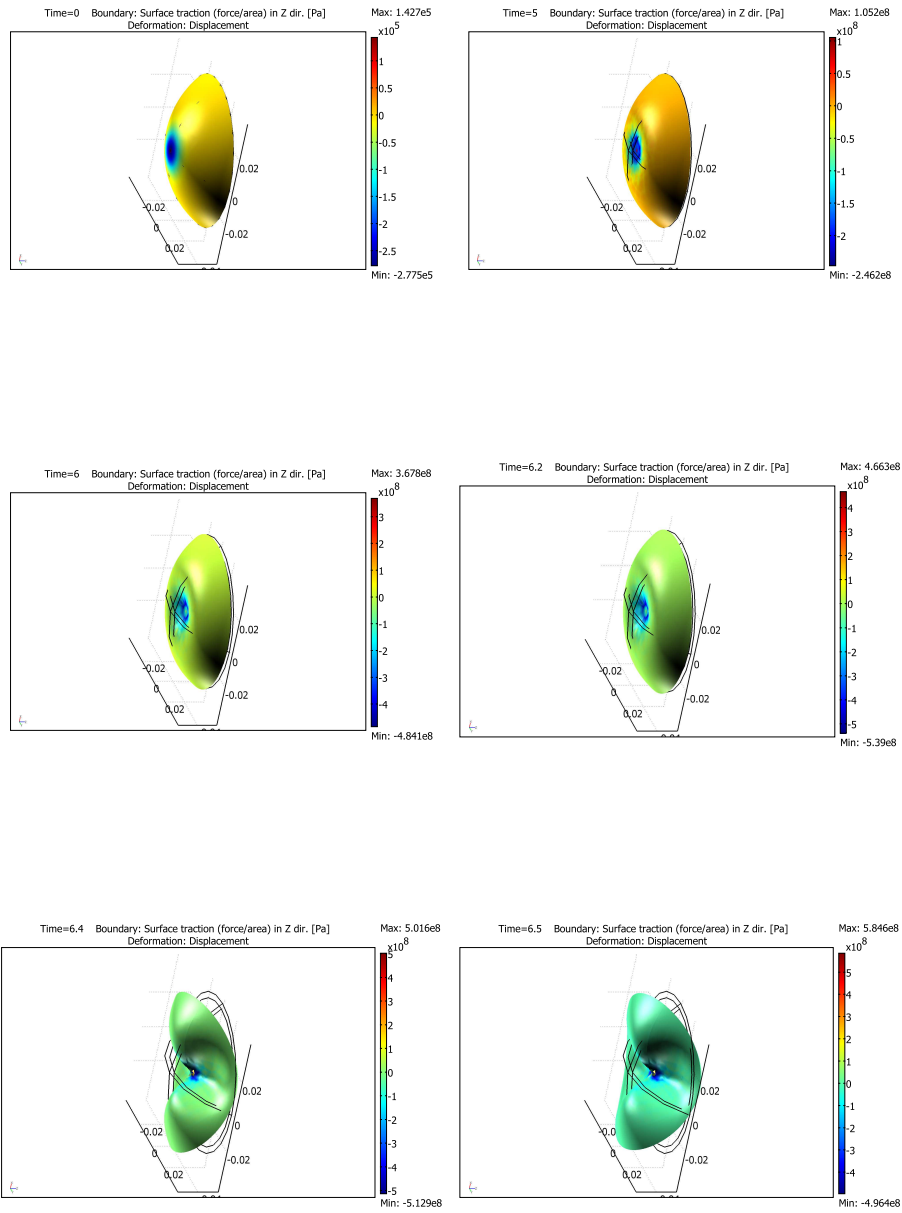
Figure 14: Inversion of the half-half-sphere!

(a) Z displacement at apex
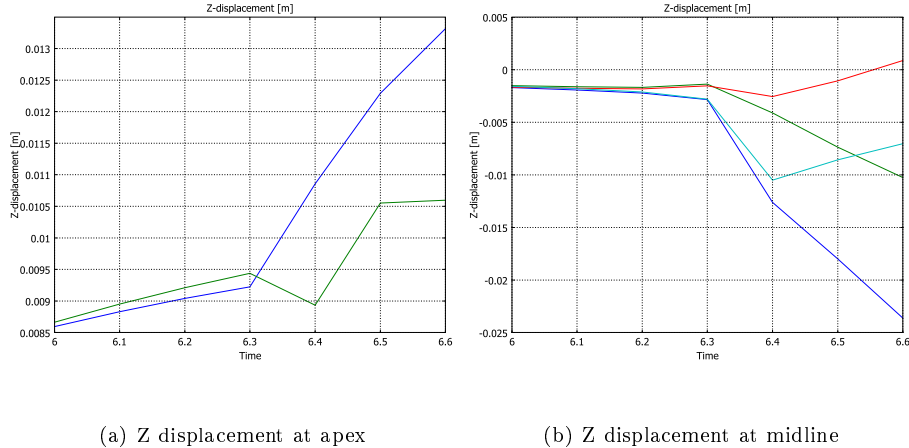
(b) Z displacement at midline

Figure 15: Displacement in the Z-direction of the (i) apical and (ii) circumferential points during the dynamic portion of the inversion process.

and viscosity. Comparison with discrete truss model may be useful, and would account for cytoplasmic bridges more accurately.

More generally, this project has spawned an interest in modeling membranes. While much work has been done on this area using thin shell approximations, I am interested to see if thin, but still three-dimensional FEM simulations can correctly model their behavior. During the course of this work, several membrane models that were not shown here were created to help me understand the capability of FEM in this area. The biggest question is if computation is cheap, why not use 3D FEM and not use the complicated thin shell approximation?

Experimentally, I am also interested in doing some rheological studies of the epithelial sheets. Finding a realistic set of parameters would be useful here, and the creep, relaxation, and cyclic tests could be performed. I intended to contact David Weitz's group to see if I can use their equipment.

The obvious bifurcation points in the time-dependent solutions are also of interest. The interplay between the geometry, the material model, and the time step needs more investigation. Consultation of a dynamical systems text will be my next step in this area. While inertia plays a small role in both the rubber ball, and the *Volvox*, it was interesting to find that solving the time-dependent problem helped to find the unstable solutions we observed in some of the rubber models.

Once the issues of reality versus model have been resolved, and we are able to properly simulate the wild-type and a mutant or two, we can apply the model to the many other inversion types in other species of *Volvox*, as shown in figure 16. Once proved, this type of analysis can be useful for understanding more epithelial sheet folding problems, such as that in gastrulation, neural tube

formation, and many other processes in "higher" organisms, such as ourselves.

References

[1] Douglas G Cole and Mark V Reedy. Algal morphogenesis: how volvox turns itself inside-out. *Curr Biol*, 13(19):R770–R772, Sep 2003.

[2] Armin Hallmann. Morphogenesis in the family volvocaceae: different tactics for turning an embryo right-side out. *Protist*, 157(4):445–461, Oct 2006.

[3] G. W. Ireland and S. E. Hawkins. Inversion in volvox tertius: the effects of con a. *J Cell Sci*, 48:355–366, Apr 1981.

[4] D. Kirk. *Volvox*. Cambridge University Press, 1998.

[5] D. L. Kirk and J. F. Harper. Genetic, biochemical, and molecular approaches to volvox development and evolution. *Int Rev Cytol*, 99:217–293, 1986.

[6] Ghazaleh Nematollahi, Arash Kianianmomeni, and Armin Hallmann. Quantitative analysis of cell-type specific gene expression in the green alga volvox carteri. *BMC Genomics*, 7:321, 2006.

[7] I. Nishii and S. Ogihara. Actomyosin contraction of the posterior hemisphere is required for inversion of the volvox embryo. *Development*, 126(10):2117–2127, May 1999.

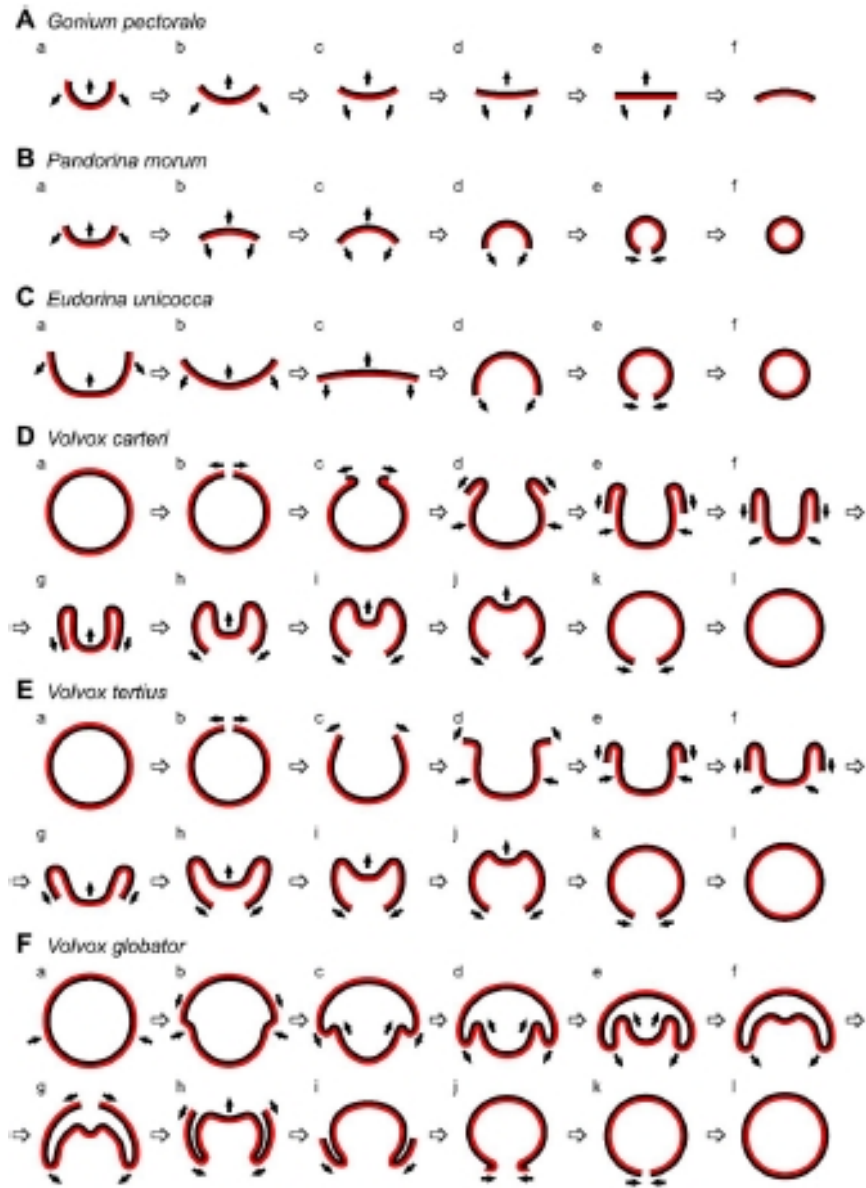[8] Ichiro Nishii, Satoshi Ogihara, and David L Kirk. A kinesin, inva, plays an essential role in volvox morphogenesis. *Cell*, 113(6):743–753, Jun 2003.

Figure 16: Schematic of inversion in other Volvocaceans.